Nuclear Medicine and Biology 42 (2015) 123–130

Contents lists available at ScienceDirect

Nuclear Medicine and Biology

journal homepage: www.elsevier.com/locate/nucmedbio

Radiolabeling and biological evaluation of the GX1 and RGD-GX1 peptide sequence for angiogenesis targeting

E.A. Oliveira *, B.L. Faintuch

Radiopharmacy, Institute of Energy and Nuclear Research, Sao Paulo, SP, Brazil, Av. Prof. Lineu Prestes, 2242 05508-000 São Paulo, SP, Brazil

ARTICLE INFO

Article history:
Received 3 July 2014
Received in revised form 3 September 2014
Accepted 15 September 2014

Keywords:
RGD and GX1 peptides
Technetium-99 m
Angiogenesis

ABSTRACT

Introduction: Aiming to develop a novel ^{99m}Tc-labeled imaging agent, for angiogenesis and tumor receptors, two peptides obtained from phage display library, namely GX1 and the heterodimer RGD-GX1, were synthesized in a cyclic conformation. They were radiolabeled with ^{99m}Tc, employing the HYNIC chelator, for radiochemical evaluation and biological properties.

Methods: Radiolabeling, radiochemical control, plasma protein binding, and partition coefficient were assessed for both radioconjugates. Biodistribution in healthy Balb/c mice was carried out, in order to evaluate the biological behaviour of the radiocomplexes.

Results: The conjugates displayed a rather similar pharmacokinetic profile. They were prepared with high radiochemical purity (>96%), and both were hydrophilic (log P of −2.25 and −2.51 respectively). Preferential renal excretion was observed. Kidney uptake (42.31 ± 5.35 %ID/g) for ^{99m}Tc-HYNIC-E-[c(RGDfk)-c(GX1)], 1 h post-injection was about three times higher than the uptake of ^{99m}Tc-HYNIC-PEG$_4$-c(GX1) (11.92 ± 4.77%ID/g). Total blood, bone and muscle values revealed a slightly slower clearance for the RGD-GX1 radiocomplex.

Conclusion: The high radiochemical purity achieved, and the similar *in vivo* profile observed for both radioconjugates, make them potential candidates for radiopharmaceuticals for tumor imaging. Further investigations of binding affinity, and uptake of GX1 and RGD-GX1 peptides in tumor models, are warranted.

1. Introduction

New radiopharmaceuticals with ability to improve the diagnostic and therapeutic strategies for diseases that affect the population are desirable, and the most important target is cancer [1].

Cancer has high mortality rate, partly due to the lack of convenient screening tests for early diagnosis, as well as tumor-specific drug delivery systems. Currently, most of the drugs for cancer do not fully differentiate between tumor and healthy cells, leading to systemic toxicity, and adverse side effects. The pursuit of peptides which specifically recognize tumor cells, and tumor vasculature, has been carried out over the years [2].

Through phage display technology, many tumor homing peptides have been discovered, with potential to detect cancer *in vivo*, and deliver anticancer agents specifically to the tumor site. Nowadays, several tumor homing peptides are being tested for diagnosis and therapy in various phases of clinical trials [2].

Radiolabelled peptides with affinity to receptors expressed in tumor cells tend to exhibit rapid tissue penetration and low antigenicity. Their easy availability and rapid clearance from blood and other non-target tissues are further advantages [3].

Angiogenesis, the physiological process of new blood vessel formation, is a crucial step in cancer growth, because it supplies the tumor with oxygen and nutrients. Also it increases the risk of metastasis, allowing cells which have left the original site and spread via lymphatic or the bloodstream, to generate distant secondary malignancies [4,5].

Through *in vivo* screening of a phage-display peptide library, it was previously recognized the affinity of the RGD and the GX1 (CGNSNPKSC) peptides with angiogenesis receptors [6,7]. The RGD motif has been well studied, being known for its binding specificity to integrin receptors, especially integrin αVβ3, which is present in angiogenesis and also in tumors [8–12].

The GX1 motif is a novel peptide, used as a vascular marker in cancer. Recent studies suggest affinity with integrin α3β1 for tumor targeting and imaging [13–17]. The creation of a heterodimer formed by two different peptides, can improve tumor cell affinity, by means of binding to two different kinds of receptors.

The radionuclide attached to the molecule defines the diagnostic or therapeutic character of the radiopharmaceutical. An important feature of radiopharmaceuticals for cancer is to accumulate only in the tumor area, in order to achieve the required result, with damage minimization to healthy tissues [18]. In this setting, the Technetium radioisotope, in its metastable form, has been widely used in nuclear medicine imaging. Technetium-99 m has ideal physical properties for image acquisition and patient safety, such as short half-life of 6 h, and gamma-photo emission of a single energy at 140 keV. Also, its use is facilitated due to commercially available generators of ^{99}Mo/^{99m}Tc, and the chemical properties that render easy and quick the radiolabeling of a large variety of molecules [19].

* Corresponding author. Tel.: +55 11 31339531; fax: +55 11 31338956.
E-mail address: ericaoliveira@usp.br (E.A. Oliveira).

http://dx.doi.org/10.1016/j.nucmedbio.2014.09.004
0969-8051/

The radiolabeling can be conducted with the help of a chelator, namely HYNIC (6-Hydrazinonicotinic acid), which is widely used to increase the stability and accelerate excretion, with lower accumulation in the body [20–23].

The purpose of this study was to evaluate the radiochemical and biological properties of the GX1 peptide alone, and of the heterodimer RGD-GX1 radiolabeled with ^{99m}Tc. They were commercially synthesized with the chelator (HYNIC), and designed in a cyclic conformation [Figs. 1 and 2], in order to improve binding ability and excretion. The establishment of the pharmacokinetic profile of both radiopharmaceuticals will enable to plan future studies in tumor models.

2. Methods

2.1. Radiolabeling

Preparation and labeling procedures were identical for both peptides, and all solutions were nitrogen-purged. In brief, it was added to a sealed reaction vial 20 mg of tricine and 5 mg of EDDA (ethylenediamine-N,N'-diacetic acid), dissolved in phosphate buffer 0, 1 N, 10 μL of HYNIC-PEG$_4$-c(GX1) 774.9 μM or HYNIC-E-[c(RGDfk)-c(GX1)] 569.5 μM (μg/mL) (CPC Scientific Inc., CA, USA), stannous chloride in HCl solution 0.1 M, and 500 μL of Na^{99m}TcO$_4$ (1850 MBq) (^{99}Mo/^{99m}Tc generator from Institute of Energy and Nuclear Research, Sao Paulo, SP, Brazil). Reaction was induced by heating at 100 °C for 20 min, subsequently cooled to room temperature. All reagents were acquired from Merck and Sigma–Aldrich (Sao Paulo, Brazil).

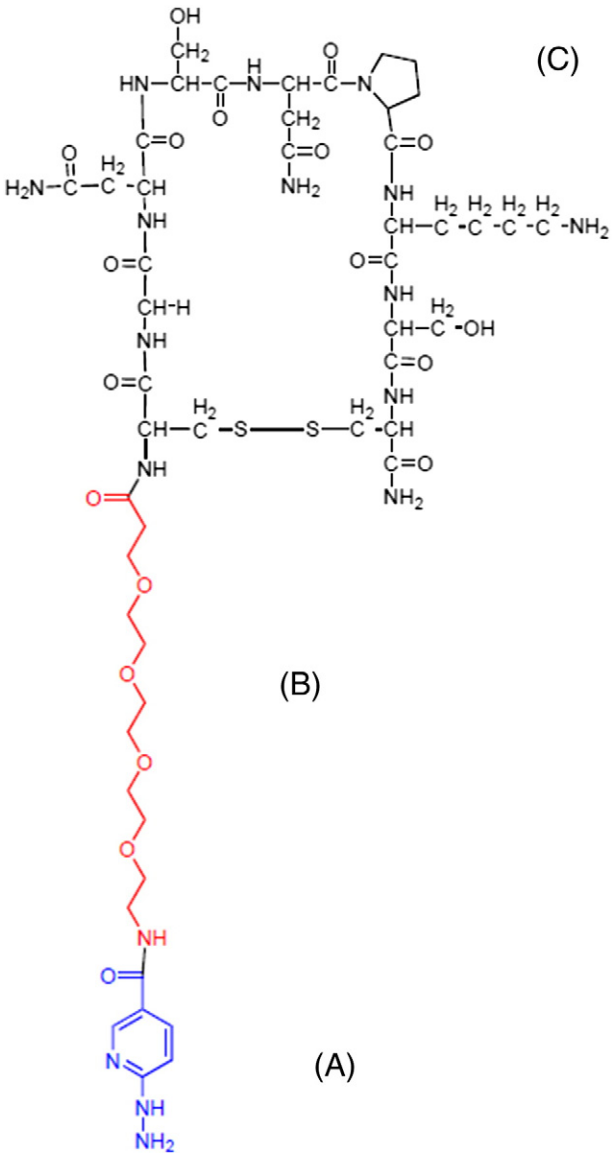

Fig. 1. Structural formula of HYNIC-PEG$_4$-c(GX1) molecular weight: 1290.4, (A) HYNIC; (B) PEG$_4$; (C) GX1 cyclic peptide.

2.2. Radiochemical control

Radiochemical evaluation of ^{99m}Tc-HYNIC-PEG$_4$-c(GX1) and ^{99m}Tc-HYNIC-E-[c(RGDfk)-c(GX1)] was performed by instant thin layer chromatography (ITLC), using silica gel strips (ITLC-SG, Gelman Sciences, AnnArbor, MI, USA), with a two solvent system of methylethylketone and acetonitrile 50%. Results from ITLC experiments were confirmed by reverse phase high performance liquid chromatography (1260 Infinity HPLC system, Agilent Technologies Inc., Santa Clara, CA, USA), using a C18 column (5.0 mm, 100A°, 4.6 x 250 mm, Waters, Milford, MA, USA) and a flow rate of 1.0 mL/min. The solvent system consisted of H_2O containing 0.1% trifluoracetic acid (solvent A) and acetonitrile containing 0.1% trifluoracetic acid (solvent B). The HPLC gradient system began with a solvent composition of 95% A and 5% B, and followed a linear gradient of 30% A:70% B from 0 to 25 min, and 5% A:95% B from 25 to 30 min. UV absorption of products was measured at 280 nm.

2.3. Partition coefficient

A small amount (100 μL) of each radiotracer was added to a mixture of equal volumes of water and octanol. The tubes with the mixture were vigorously vortexed over a period of 15 min, and centrifuged at 5000 × g for 3 min. Samples (in triplicate) from both phases were collected, and measured in a gamma radioactivity counter, enabling *log P* values to be calculated.

2.4. Plasma protein binding

The percentage of the radioconjugates bound to plasma proteins was evaluated by the precipitation method. Blood samples were obtained from healthy Balb/c mice, under anesthesia at 5, 60 and 120 min p.i. of ^{99m}Tc-labeled conjugates. Aliquots were collected from the heart in heparinized tubes, and centrifuged (1877 × g) for 15 min at room temperature. One mL of trifluoroacetic acid 10% (TCA) was added to plasma and centrifuged (2815 × g) for 15 min at 4 °C. Then the supernatant was discarded, and the procedure was repeated three times. The pellet was taken for gama-counting along with the standard, which corresponded to intact plasma. The experiments were conducted in triplicate.

2.5. In vitro serum stability

The *in vitro* stability of the ^{99m}Tc-labeled tracers was evaluated at different time points using the following procedure: 100 μL of ^{99m}Tc-HYNIC-PEG$_4$-c(GX1) or ^{99m}Tc-HYNIC-E-[c(RGDfk)-c(GX1)] was added to 1 mL of fresh human serum at 37 °C. Aliquots were withdrawn during the incubation at different time intervals till 4 h. The supernatant was subjected to HPLC using the same system used for quality control. Increases in the free pertechnetate were considered for the degree of degradation.

2.6. In vivo studies

Experiments were carried out in compliance with the guidelines for animal experimentation, Scientific Ethics Committee, IPEN/CNEN-SP. Biodistribution of ^{99m}Tc-HYNIC-PEG$_4$-c(GX1) and ^{99m}Tc-HYNIC-E-[c(RGDfk)-c(GX1)] was conducted in healthy Balb/c mice (n = 5), at different times (5 min, 30 min, 1 h, 2 h, 4 h, 6 h and 24 h), post injection of the radiotracers. Animals were injected with the radiolabeled complex (0.05 mL/18.5 MBq) via the tail vein. All urethane-anesthetized animals

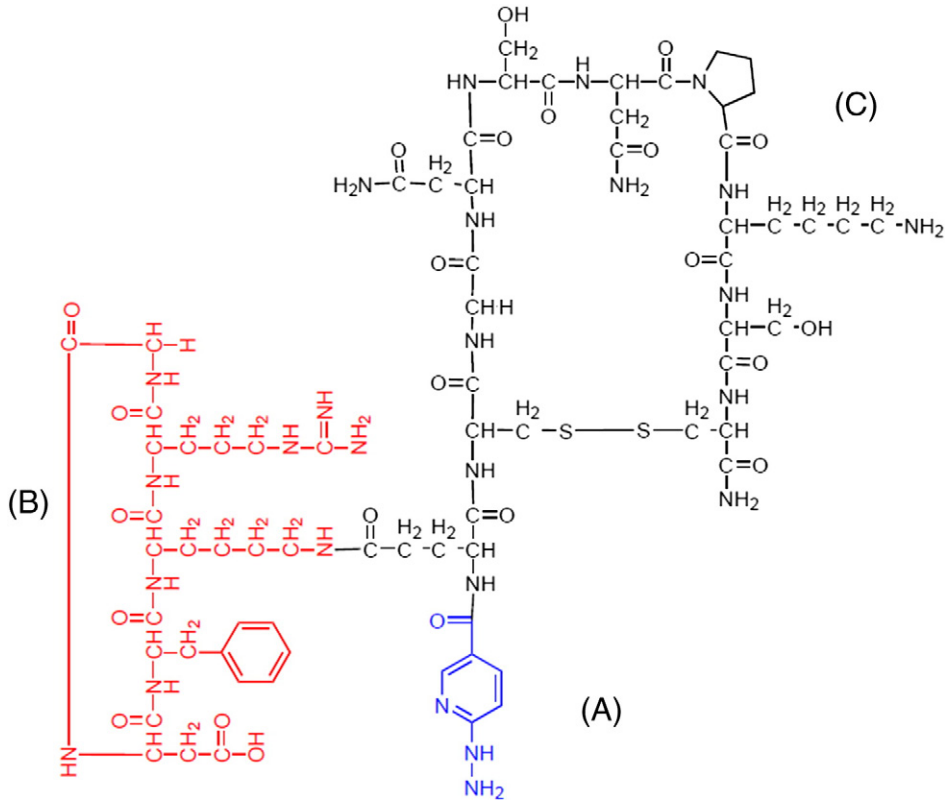

Fig. 2. Structural formula of HYNIC-E-[c(RGDfk)-c(GX1)] molecular weight: 1755.9, (A) HYNIC; (B) RGDfk cyclic peptide; (C) GX1 cyclic peptide.

were sacrificed by cervical dislocation, and organs and tissues of interest were harvested, weighed and counted. The radioactivity in each organ was expressed as percentage of the injected dose per gram of organ (%ID/g). Total blood, muscle and bone uptake was calculated, assuming 7%, 40% and 10% of total body weight, respectively.

2.7. In vitro cell binding assay

Human umbilical vein endothelial cells (HUVEC) were grown in RPMI (Roswell Park Memorial Institute-1640 Medium). Cells (5×10^5/well) were seeded into well culture plates, and it was added the radiotracers ^{99m}Tc-HYNIC-PEG$_4$-c(GX1) or ^{99m}Tc-HYNIC-E-[c(RGDfk)-c(GX1)] (0.15 mCi/well). For nonspecific binding assays, cold conjugate (1 mmol/L/well) was also added. After incubation at 37 °C for 5, 30, 60, 90, and 120 min, cells were rinsed, for determination of surface-bound and internalization of the radioligand. Studies were performed in triplicate (n = 3).

2.8. Statistical analysis

All data were expressed as mean ± standard deviation (SD). Student's t test was used for comparisons, and $p < 0.05$ was considered statistically significant.

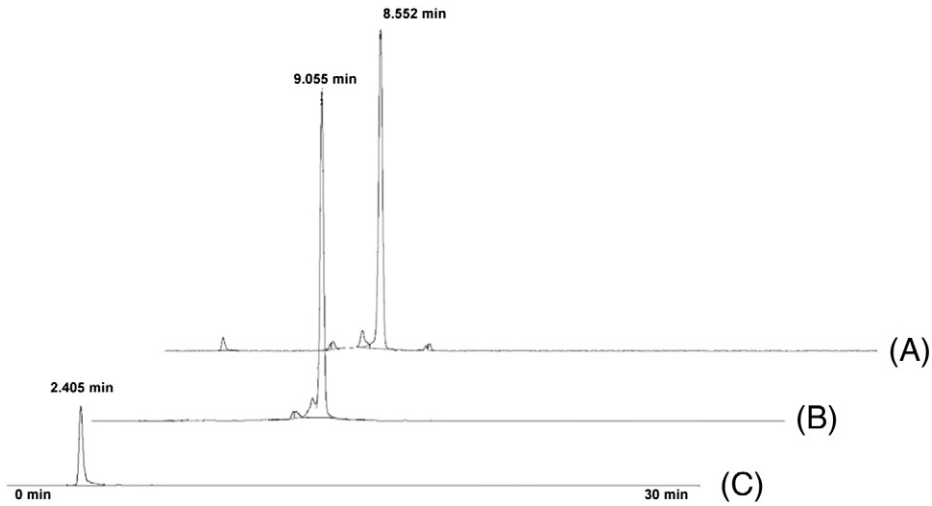

Fig. 3. Radiochromatograms: (A) ^{99m}Tc-HYNIC-PEG$_4$-c(GX1); (B) ^{99m}Tc- HYNIC-E-[c(RGDfk)-c(GX1)]; (C) $^{99m}TcO_4^-$.

Table 1
Plasma protein binding of ^{99m}Tc-HYNIC-PEG$_4$-c(GX1) and ^{99m}Tc-HYNIC-E-[c(RGDfk)-c(GX1)] (n = 3).

		5 min	1 h	2 h
% of plasma protein binding	GX1	12.74 ± 6.92	17.62 ± 2.15*	99.24 ± 0.23*
	RGD-GX1	23.73 ± 8.20	34.25 ± 4.01*	54.87 ± 5.49*

* $p < 0.05$ between GX1 and RGD-GX1 at the same time and analysis.

3. Results

Radiolabeling of the conjugates was done with a specific activity of 238.74 MBq/nmol for ^{99m}Tc-HYNIC-PEG$_4$-c(GX1) and 324.84 MBq/nmol for ^{99m}Tc-HYNIC-E-[c(RGDfk)-c(GX1)]. Radiochemical purity was 98.83 ± 0.87% and 96.06 ± 1.83% respectively, obtained by ITLC. The retention time (t_R) of 8.552 min and 9.055 min, can be observed in HPLC radiochromatogram [Fig. 3], as well the small peak of ion $^{99m}TcO_4^-$, with a retention time (t_R) of 2.405 min.

Mean value of the partition coefficient (*log P*) was −2.51 ± 0.04 for ^{99m}Tc-HYNIC-PEG$_4$-c(GX1) and −2.25 ± 0.07 for ^{99m}Tc-HYNIC-E-[c(RGDfk)-c(GX1)], with statistical significance ($p < 0.05$). Both results are within the range of hydrophilicity.

Both radiotracers had an increased binding to plasma proteins with time, reaching at 2 h 99.24 ± 0.23% and 54.87 ± 5.49% for ^{99m}Tc-HYNIC-PEG$_4$-c(GX1) and ^{99m}Tc-HYNIC-E-[c(RGDfk)-c(GX1)], respectively [Table 1]. Despite the high values, these percentages represents only 0.07 ± 0.03% and 0.14 ± 0.00%, respectively, of the total injected dose in the precipitated plasma [Fig. 4], indicating that the vast majority of the products had already cleared the blood system.

The complexes showed excellent *in vitro* stability under physiological conditions in human serum remaining intact after 4h. Consequently, no reoxidation to pertechnetate was observed, as indicated by HPLC controls [Figs. 5 and 6].

The radioconjugates showed a comparable distribution pattern for most organs. Remarkable blood uptake was observed at the earliest time point (5 min) for both radiotracers, decreasing after 30 min to approximately 73.3% and 46.8% for ^{99m}Tc-HYNIC-PEG$_4$-c(GX1) and ^{99m}Tc-HYNIC-E-[c(RGDfk)-c(GX1) respectively. Both radiotracers were cleared approximately 93% from blood but more slowly for the second radiotracer [Fig. 7].

The uptake of ^{99m}Tc-HYNIC-E-[c(RGDfk)-c(GX1)] by kidneys at 1 h was a little more than three times higher than for ^{99m}Tc-HYNIC-PEG$_4$-c(GX1) (42.31 ± 5.35 %ID/g and 11.92 ± 4.77 %ID/g) [Figs. 8 and 9]. Liver uptake was very similar for both radiotracers at 5 min, 2.74 ± 0.88 %ID/g for ^{99m}Tc-HYNIC-PEG$_4$-c(GX1), and 2.73 ± 0.20 %ID/g for ^{99m}Tc-HYNIC-E-[c(RGDfk)-c(GX1)].

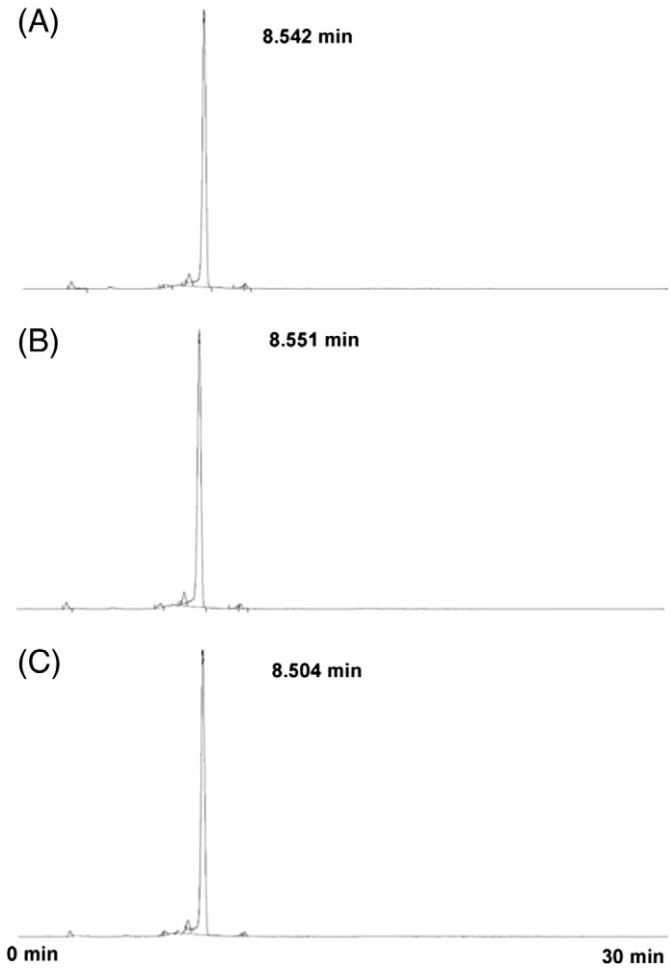

Fig. 5. Serum stability of ^{99m}Tc-HYNIC-PEG$_4$-c(GX1) at (A)1 h; (B) 2 h and (C) 4 h.

The uptake of ^{99m}Tc-HYNIC-E-[c(RGDfk)-c(GX1)] in small (6.21 ± 1.27 %ID/g) and large intestine (6.34 ± 2.02 %ID/g) had values more than two times higher than for ^{99m}Tc-HYNIC-PEG$_4$-c(GX1), in the same small (2.73 ± 0,81 %DI/g) and large bowel (2.63 ± 1.03 %ID/g) at 5 min p.i., followed by a constant decrease in the course of time.

In other organs, the highest uptakes of the radiotracers were observed in lungs, followed by spleen and stomach at 5 min p.i., as demonstrated in Table 2. The uptake in %ID/g of the radiotracers, diminished

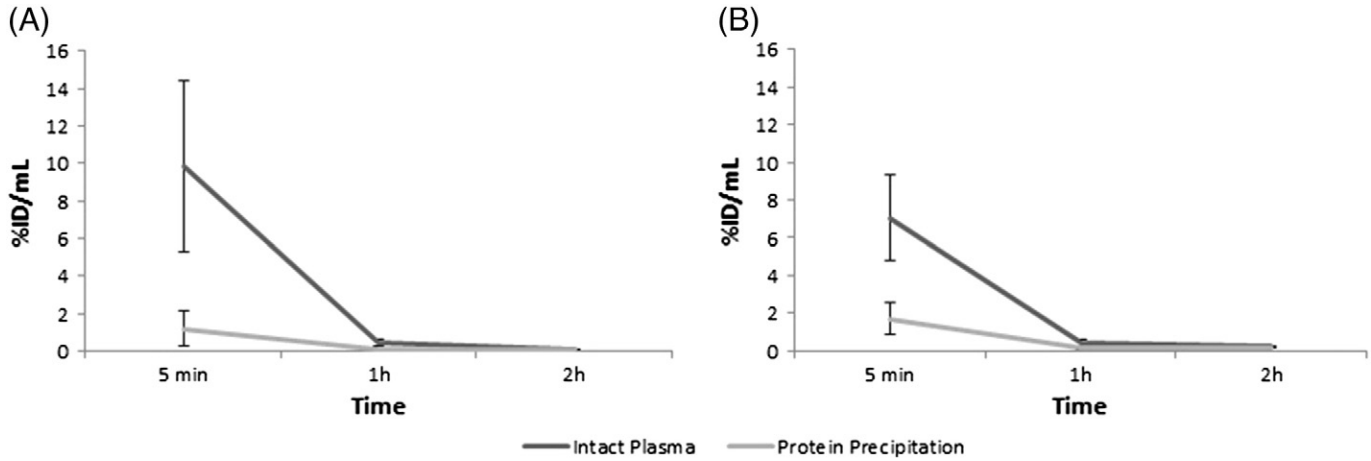

Fig. 4. Plasma protein binding analysis (A) ^{99m}Tc-HYNIC-PEG$_4$-c(GX1); (B) ^{99m}Tc- HYNIC-E-[c(RGDfk)-c(GX1)].

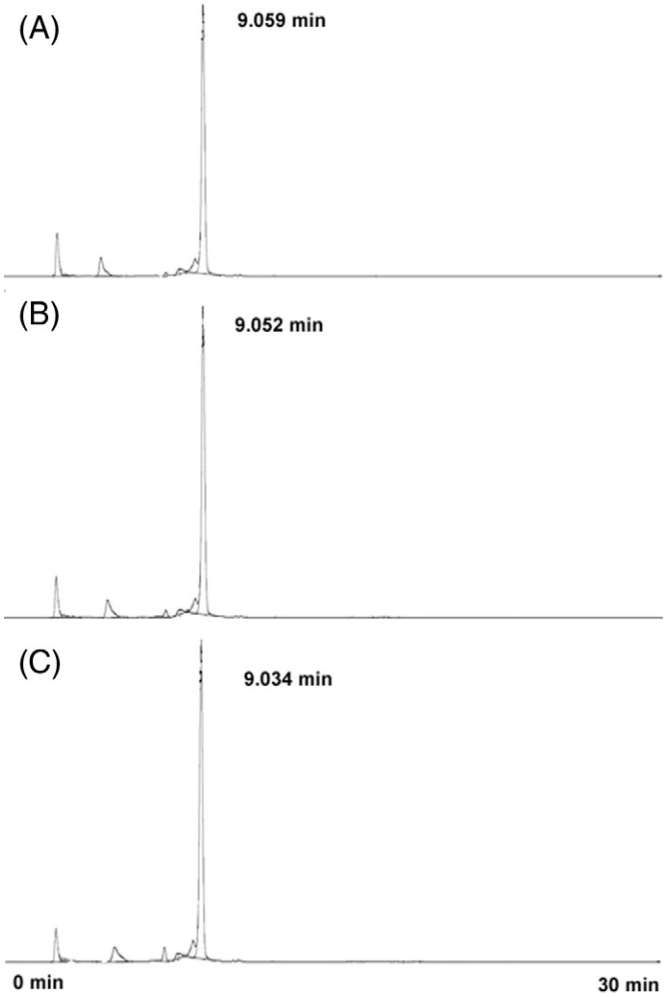

Fig. 6. Serum stability of ^{99m}Tc- HYNIC-E-[c(RGDfk)-c(GX1)] at (A)1 h; (B) 2 h and (C) 4 h.

one hour post injection to less than 3% of the injected dose, excepted by stomach and spleen in ^{99m}Tc-HYNIC-E-[c(RGDfk)-c(GX1)] injected mice, subsequently remaining around 2% in longer times. In synthesis, the RGD-GX1 radiotracer had slower clearance and higher uptake in tested organs. Brain uptake was very low for both radiotracers, even at the first time of 5 min.

Percentages of total blood, muscle and bone are displayed in Table 3. Both radioconjugates exhibited similar accumulation at blood, muscle

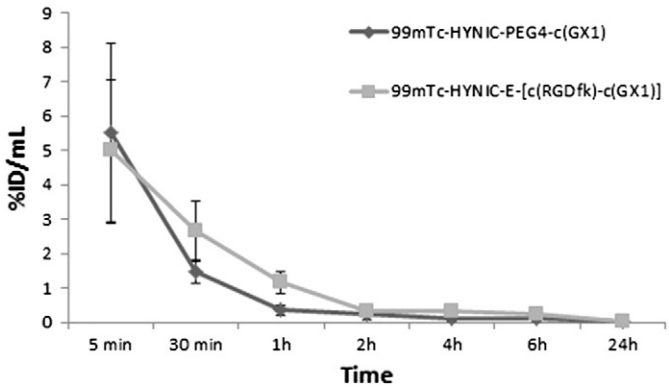

Fig. 7. Blood depuration in Balb/c mice. The values are express in %ID/mL (0.05 mL/18.5 MBq).

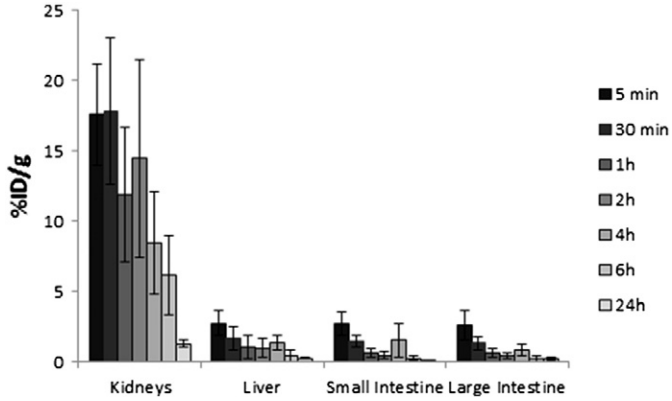

Fig. 8. Excretion organ uptake of ^{99m}Tc-HYNIC-PEG4-c(GX1) in Balb/c mice (0.05 mL/18.5 MBq). The radioactivity in the intestines was evaluated after thoroughly removing the luminal contents.

and bone after 5. ^{99m}Tc-HYNIC-PEG$_4$-c(GX1) quickly cleared and reached very low levels within 1 h p.i. Although the clearance pattern of the two radiocomplexes was rather similar, clearance of ^{99m}Tc-HYNIC-E-[c(RGDfk)-c(GX1)] was slower, reaching negligible levels only at 24 h p.i. for total muscle and bone.

In vitro studies with HUVEC cells are displayed at Fig. 10. Total binding of ^{99m}Tc-HYNIC-PEG$_4$-c(GX1) had a peak at 60 min of incubation (0.41 ± 0.04%), and approximately 51% of the tracer was internalized at 5 min. In contrast, with ^{99m}Tc-HYNIC-E-[c(RGDfk)-c(GX1)], total binding reached the highest value at 120 min of incubation (0.35 ± 0.07%), and also internalization increased with the incubation time, reaching 54% at 120 min.

4. Discussion

Peptides are endowed with much importance in receptor targeting of tumors, due to favorable features when compared to other agents like monoclonal antibodies and their derivatives [24–27].

Such molecules are often disease-specific due to their purposeful design, primarily targeting receptors. In this preliminary study, the radiotracers aimed instead a pathophysiological process, namely angiogenesis, however one that is strongly expressed by rapidly growing lesions, thus representing a surrogate for cancer development. In the future, these radiotracers will be evaluated in actual tumor models.

The cores of the molecules are the peptides, nominally GX1 and RGD. Both were selected by phage display technology, a useful tool for identifying specific peptide sequences for known receptors [28].

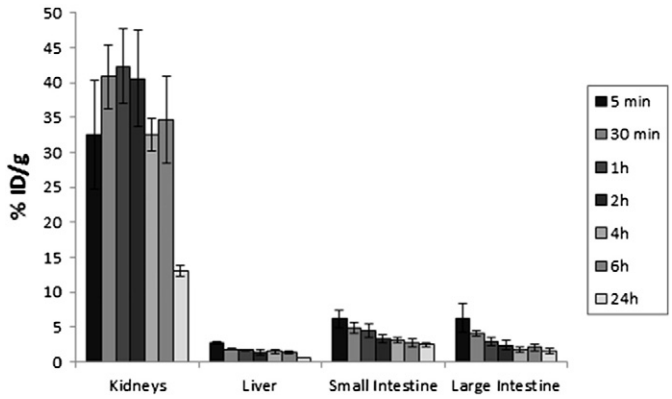

Fig. 9. Excretion organ uptake of ^{99m}Tc-HYNIC-E-[c(RGDfk)-c(GX1)] in Balb/c mice (0.05 mL/18.5 MBq). The radioactivity in the intestines was evaluated after thoroughly removing the luminal contents.

Table 2
Biodistribution of ^{99m}Tc-HYNIC-PEG$_4$-c(GX1) and ^{99m}Tc-HYNIC-E-[c(RGDfk)-c(GX1)] in healthy mice (%ID/g ± SD).

Organ/Time		5 min	30 min	1 h	2 h	4 h	6 h	24 h
Heart	GX1	2.74 ± 0.69	1.31 ± 0.38	0.55 ± 0.34	0.35 ± 0.29	0.08 ± 0.04	0.06 ± 0.03	0.02 ± 0.01
	RGD-GX1	2.68 ± 0.64	1.44 ± 0.28	0.85 ± 0.18	0.46 ± 0.07	0.40 ± 0.02	0.45 ± 0.08	0.27 ± 0.03
Lungs	GX1	6.13 ± 1.40	2.97 ± 0.64	1.14 ± 0.59	0.78 ± 0.54	0.18 ± 0.11	0.16 ± 0.09	0.04 ± 0.01
	RGD-GX1	5.79 ± 1.73	3.53 ± 0.72	2.57 ± 0.25	1.16 ± 0.19	0.97 ± 0.09	1.00 ± 0.13	0.73 ± 0.32
Spleen	GX1	3.01 ± 1.15	1.33 ± 0.30	0.75 ± 0.39	0.39 ± 0.19	0.19 ± 0.06	0.20 ± 0.10	0.04 ± 0.01
	RGD-GX1	4.31 ± 1.15	3.70 ± 0.38	2.39 ± 0.65	2.54 ± 0.29	1.97 ± 0.42	2.58 ± 0.71	2.20 ± 0.22
Stomach	GX1	2.30 ± 0.39	1.77 ± 0.69	0.55 ± 0.35	1.38 ± 0.86	1.26 ± 0.06	0.59 ± 0.40	0.15 ± 0.02
	RGD-GX1	2.25 ± 0.26	2.05 ± 0.64	1.43 ± 0.34	2.09 ± 0.26	2.20 ± 0.24	2.26 ± 0.63	1.11 ± 0.09
Pancreas	GX1	2.28 ± 0.62	1.16 ± 0.49	0.77 ± 0.37	0.32 ± 0.24	0.10 ± 0.06	0.08 ± 0.05	0.03 ± 0.03
	RGD-GX1	2.76 ± 0.64	1.30 ± 0.28	0.98 ± 0.13	0.50 ± 0.13	0.41 ± 0.04	0.43 ± 0.05	0.24 ± 0.02
Muscle	GX1	1.36 ± 0.37	0.73 ± 0.35	0.26 ± 0.17	0.18 ± 0.16	0.08 ± 0.05	0.05 ± 0.02	0.01 ± 0.00
	RGD-GX1	1.17 ± 1.10	0.85 ± 0.12	0.61 ± 0.16	0.28 ± 0.02	0.24 ± 0.01	0.26 ± 0.07	0.18 ± 0.03
Bone	GX1	2.24 ± 0.69	1.52 ± 0.83	0.61 ± 0.42	0.36 ± 0.18	0.27 ± 0.19	0.24 ± 0.16	0.03 ± 0.01
	RGD-GX1	2.51 ± 0.31	2.43 ± 0.74	1.61 ± 0.35	0.90 ± 0.15	0.72 ± 0.06	0.98 ± 0.15	0.68 ± 0.16
Brain	GX1	0.30 ± 0.12	0.14 ± 0.08	0.06 ± 0.04	0.05 ± 0.04	0.02 ± 0.02	0.02 ± 0.02	0.00 ± 0.00
	RGD-GX1	0.30 ± 0.06	0.15 ± 0.03	0.11 ± 0.02	0.06 ± 0.02	0.07 ± 0.05	0.06 ± 0.01	0.03 ± 0.01

Linear peptides are recognized as more susceptible to degradation *in vivo*, with short half-life. That could impair diagnostic ability, and even be associated with adverse effects during treatment, imaging, and general biological applications. Cyclization has thus represented an alternative, to improve the binding properties of peptides [7,13,29–31].

The option for ^{99m}Tc was based on chemical, physical and nuclear properties, as well as cost and diagnostic energy. Nevertheless, to link the peptide and get a stable *in vivo* radiotracer, a chelator agent is required.

A variety of bifunctional chelators is available for labeling proteins, peptides, and other biologically active molecules by ^{99m}Tc [32–34].

HYNIC (6-Hydrazinonicotinic acid) was considered the best candidate in the light of high specific labeling activity, favorable stability, and low accumulation in the body. In association with various coligands, it permits control of the hydrophilicity and pharmacokinetics of the labeled peptide [20–23,35–37].

Coligands are necessary to complete the coordination sphere of the technetium core, because HYNIC may only occupy one or two coordination positions of the radionuclide [38]. Among available coligands, tricine and EDDA (ethylenediamine diacetic acid) tend to promote the best radiolabeling efficiency. Pegylation was also used in one molecule, GX1, aiming at improved pharmacokinetics, despite the possibility of creating steric hindrance. This insertion was not possible in the other molecule (RGD-GX1), precisely because of a steric barrier.

The design of dual molecular targeting is an attractive approach, because many cancer types simultaneously express multiple receptors [39]. That was the rationale behind the dimer RGD-GX1. Indeed, the RGD peptide has been previously associated with other peptides, creating heterodimers such as Bombesin-RGD and RGD-αMSH (melanocyte-stimulating hormone), with the objective of improving tumor cell affinity, by means of binding to two different receptors [40–43].

Radiolabeling in the current experience was easy and fast. HPLC analysis confirmed a single peak for each of the tracers, suggesting that only one product was formed, without isomers, with high radiochemical purity, high serum stability and needless of purification steps. Values of retention time and partition coefficient were in the same range for both complexes, matching similar molecular size and hidrophilicity pattern.

The rapid excretion profile, predominantly via the urinary tract, along with liver and intestine uptake, is consistent with the hydrophilic partition coefficient of both radiotracers. Nonetheless, a significant percentage of radioactivity in the hepatobiliary tract remained, indicating the importance of this path for total elimination of the radioactive complex. Lipophilicity is considered undesirable in a radiopharmaceutical because it leads to intestinal instead of renal clearance. Yet, secondary metabolization of the product in the digestive tract could still result in release of radionuclide into the bloodstream, in forms which undergo renal elimination [44].

Blood clearance was rapid, and the washout of GX1 was typically higher than that of RGD-GX1. The larger molecule could be responsible for the slower excretion of ^{99m}Tc-HYNIC-E-[c(RGDfk)-c(GX1)].

The results of total blood and total plasma binding support the hypothesis that a very minimal percentage of radioactivity remained in the circulatory system at longer times, for both radiotracers. Plasma protein binding was twice as high for the monomer tracer, probably on account of pegylation of the molecule, leading to significant inhibition of protein adsorption, less recognition by the phagocyte system, increase in the size of the molecules, and reduced glomerular filtration rate [45,46].

Most organs and tissues achieved good clearance by 60 min. As an efficient tracer should exhibit good clearance from the background tissue or blood, such results bode well for the development of clinically-relevant tracers, and this time point will be adopted for future tumor-bearing models [47].

The binding studies in HUVEC cells helped to elucidate the uptake pattern of each radiotracer. Although the uptake values were low, these were just a fraction of the potential binding, as the main target is the new vasculature, which can solely be produced *in vivo*.

5. Conclusion

Radiolabeling of GX1 and RGD-GX1 conjugates with ^{99m}Tc was successful, with high radiochemical purity. Both radiotracers were

Table 3
Percentage of total injected dose of ^{99m}Tc-HYNIC-PEG$_4$-c(GX1) and ^{99m}Tc-HYNIC-E-[c(RGDfk)-c(GX1)] in healthy Balb/c mice at different times (%ID).

Organ/Time		5 min	30 min	1 h	2 h	4 h	6 h	24 h
Blood	GX1	13.00 ± 1.25	2.62 ± 0.60	0.64 ± 0.26	0.39 ± 0.23	0.22 ± 0.14	0.25 ± 0.06	0.05 ± 0.01
	RGD-GX1	9.46 ± 4.20	5.06 ± 2.02	2.28 ± 0.65	0.62 ± 0.21	0.63 ± 0.20	0.43 ± 0.14	0.09 ± 0.02
Muscle	GX1	13.44 ± 3.91	5.17 ± 1.07	1.47 ± 0.72	0.77 ± 0.23	0.40 ± 0.13	0.37 ± 0.17	0.09 ± 0.04
	RGD-GX1	13.21 ± 2.90	9.04 ± 1.50	6.06 ± 1.08	2.86 ± 0.33	2.54 ± 0.31	2.55 ± 0.65	1.76 ± 0.31
Bone	GX1	5.53 ± 1.32	3.01 ± 1.32	0.74 ± 0.37	0.65 ± 0.24	0.46 ± 0.13	0.35 ± 0.20	0.08 ± 0.02
	RGD-GX1	6.74 ± 1.06	6.45 ± 1.92	4.38 ± 0.88	2.31 ± 0.35	1.92 ± 0.24	2.39 ± 0.32	1.67 ± 0.44

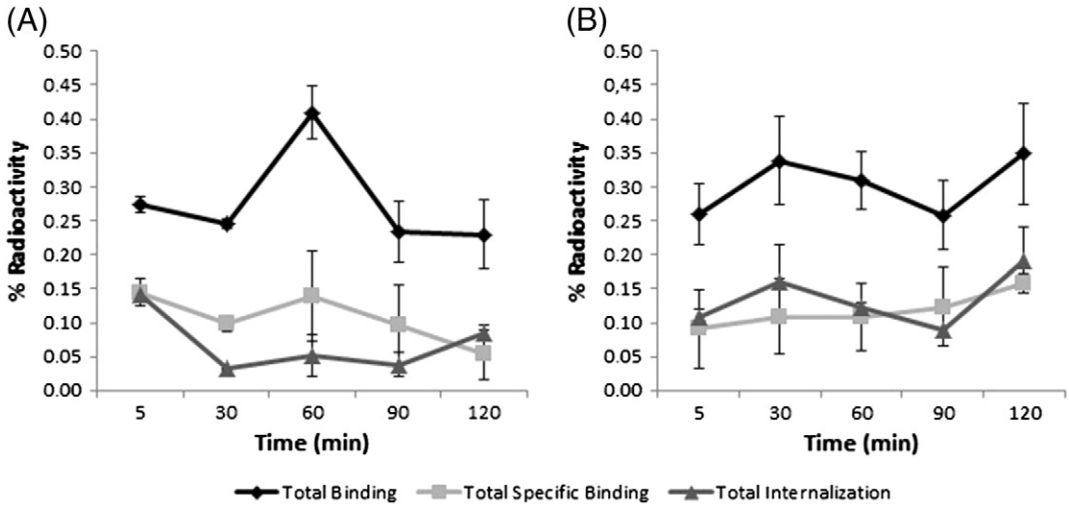

Fig. 10. Uptake binding in HUVEC cells (A) ^{99m}Tc-HYNIC-PEG$_4$-c(GX1); (B) ^{99m}Tc- HYNIC-E-[c(RGDfk)-c(GX1)].

hydrophilic with preferential renal excretion, an advantageous property for diagnostic radiopharmaceuticals. Both radioconjugates are considered potential candidates for tumor imaging, by means of nuclear medicine techniques. Further investigations of binding affinity and uptake of GX1 and RGD-GX1 peptides in tumor models are warranted.

Acknowledgements

The authors are grateful for a postgraduate Grant by Fundação de Amparo a Pesquisa do Estado de São Paulo, Brazil (Fapesp 2011/12405-0).

Appendix A. Supplementary data

Supplementary data to this article can be found online at http://dx.doi.org/10.1016/j.nucmedbio.2014.09.004.

References

[1] Psimadas D, Bouziotis P, Georgoulias P, Valotassiou V, Tsotakos T, Loudos G. Radiolabeling approaches of nanoparticles with (99 m) Tc. Contrast Media Mol Imaging 2013;8:333–9.
[2] Gautam A, Kapoor P, Chaudhary K, Kumar R, Raghava GP. Tumor homing peptides as molecular probes for cancer therapeutics, diagnostics, and theranostics. Curr Med Chem 2014;21:2367–91.
[3] Mukherjee A, Pandey U, Chakravarty R, Sarma HD, Dash A. Development of single vial kits for preparation of 68Ga-labelled peptides for PET imaging of neuroendocrine tumours. Mol Imaging Biol 2014. http://dx.doi.org/10.1007/s11307-014-0719-2.
[4] Bello L, Giussani C, Carrabba G, Pluderi M, Costa F, Bikfalvi A. Angiogenesis and invasion in gliomas. Cancer Treat Res 2004;117:263–84.
[5] Skobe M, Rockwel LP, Goldstein N, Vosseler S, Fusenig NE. Halting angiogenesis suppresses carcinoma cell invasion. Nat Med 1997;3:1222–7.
[6] Smith JW, Cheresh DA. The arg-gly-asp binding domain of the vitronectin receptor: photoaffinity crosslinking implicates amino acid residues 61-203 of the ß subunit. J Biol Chem 1988;263:18726–31.
[7] Zhi M, Wu KC, Dong L, Hao ZM, Deng TZ, Hong L, et al. Characterization of a specific phage-displayed peptide binding to vasculature of human gastric cancer. Cancer Biol Ther 2004;3:1232–5.
[8] Dijkgraaf I, Kruijtzer AW, Liu S, Soede AC, Oyen WJG, Corstens FHM, et al. Improved targeting of the avb3 integrin by multimerisation of RGD peptides. Eur J Nucl Med Mol Imaging 2007;34:267–73.
[9] Liu S, Kim YS, Hsieh WY, Sreerama SG. Coligant effect on the solution stability, biodistribution and metabolism of the 99mTc-labeled cyclic RGDfK tetramer. Nucl Med Biol 2008;35:111–21.
[10] Moncelet D, Bouchaud V, Mellet P, Ribot E, Miraux S, Franconi JM, et al. Cellular density effect on RGD ligand internalization in glioblastoma for MRI application. PLoS One 2013;8(12):e82777.
[11] Schottelius M, Wester HJ. Molecular imaging targeted receptor. Methods 2009;48:161–77.
[12] Zhang X, Xiong Z, Wu Y, Cai W, Tseng JR, Gambhir SS, et al. Quantitative PET imaging of tumor integrin alphavbeta3 expression with 18 F-FRGD2. J Nucl Med 2006;47(1):113–21.
[13] Chen B, Cao S, Zhang Y, Wang X, Liu J, Hui X, et al. A novel peptide (GX1) homing to gastric cancer vasculature inhibits angiogenesis and cooperates with TNF alpha in anti-tumor therapy. BMC Cell Biol 2009;9:10–63.
[14] Chen K, Sun X, Niu G, Ma Y, Yap I, Hui X, et al. Evaluation of 64Cu labeled GX1: a phage display peptide probe for PET imaging of tumor vasculature. Mol Imaging Biol 2012;14(1):96–105.
[15] Hu H, Yin J, Wang M, Liang C, Song H, Wang J, et al. GX1 targeting delivery of rmhTNFα evaluated using multimodality imaging. Int J Pharm 2014;461(1–2):181–91.
[16] Hui X, Han Y, Liang S, Liu Z, Liu J, Hong L, et al. Specific targeting of the vasculature of gastric cancer by a new tumor-homing peptide CGNSNPKSC. J Control Release 2008;131:86–93.
[17] Xin J, Zhang X, Liang J, Xia L, Yin J, Nie Y, et al. In vivo gastric cancer targeting and imaging using novel symmetric cyanine dye-conjugated GX1 peptide probes. Bioconjug Chem 2013;24(7):1134–43.
[18] Imam SK. Molecular nuclear imaging: the radiopharmaceuticals (review). Cancer Biother Radiopharm 2005;20(2):163–72.
[19] Banerjee S, Pillai MR, Ramamoorthy N. Evolution of Tc-99 m in diagnostic radiopharmaceuticals. Semin Nucl Med 2001;31:260–77.
[20] Decristoforo C, Faintuch-Linkowski B, Rey A, von Guggenberg E, Rupprich M, Hernandez-Gonzales I, et al. [99mTc]HYNIC-RGD for imaging integrin alphavbeta3 expression. Nucl Med Biol 2006;33:945–52.
[21] Decristoforo C, Santos I, Pietzsch HJ, Kuenstler JU, Duatti A, Smith CJ, et al. Comparison of in vitro and in vivo properties of [99mTc]cRGD peptides labeled using different novel Tc-cores. Q J Nucl Med Mol Imaging 2007;51:33–41.
[22] Janssen ML, Oyen WJ, Dijkgraaf I, Massuger LF, Frielink C, Edwards DS, et al. Tumor targeting with radiolabeled alpha(v)beta(3) integrin binding peptides in a nude mouse model. Cancer Res 2002;62:6146–51.
[23] Su ZF, He J, Rusckowski M, Hnatowich DJ. In vitro cell studies of technetium-99 m labeled RGD-HYNIC peptide, a comparison of tricine and EDDA as co-ligands. Nucl Med Biol 2003;30:141–9.
[24] Durkan K, Lambrecht FY, Unak P. Radiolabeling of bombesin-like peptide with 99mTc: 99mTc-litorin and biodistribution in rats. Bioconjug Chem 2007;18:1516–20.
[25] Okarvi SM. Peptide-based radiopharmaceuticals: future tools for diagnostic imaging of cancers and other diseases. Med Res Rev 2004;24(3):357–97.
[26] Oyen WJG, Bodei L, Giammarile F, Maecke HR, Tennvall J, Luster M, et al. Targeted therapy in nuclear medicine—current status and future prospects. Ann Oncol 2007;18:1782–92.
[27] Song KM, Lee S, Ban C. Aptamers and their biological applications. Sensors (Basel) 2012;12(1):612–31.
[28] Ueberberg S, Schneider S. Phage library-screening: a powerful approach for generation of targeting-agents specific for normal pancreatic islet-cells and islet-cell carcinoma in vivo. Regul Pept 2010;160(1–3):1–8.
[29] Dechantsreiter MA, Planker E, Mathä B, Lohof E, Holzemann G, Jonczyk A, et al. N-methylated cyclic RGD peptides as highly active and selective aVb3 integrin antagonists. J Med Chem 1999;42:3033e40.
[30] Gurrath M, Muller G, Kessler H, Aumailley M, Timpl R. Conformation/Activity studies of rationally designed potent anti-adhesive RGD peptides. Eur J Biochem 1992;210:911e21.
[31] Haubner R, Gratias R, Diefenbach B, Goodman SL, Jonzyk A, Kessler H. Structural and functional aspects of RGD-containing cyclic pentapeptides as highly potent and selective integrin aVb3 antagonists. J Am Chem Soc 1996;118:7461e72.
[32] García-Garayoa E, Maes V, Bläuenstein P, Blanc A, Hohn A, Tourwé D, et al. Double-stabilized neurotensin analogues as potential radiopharmaceuticals for NTR-positive tumors. Nucl Med Biol 2006;33(4):495–503.
[33] Maina T, Nikolopoulou A, Stathopoulou E, Galanis AS, Cordopatis P, Nock BA. [99mTc]Demotensin 5 and 6 in the NTS1-R-targeted imaging of tumours: synthesis and preclinical results. Eur J Nucl Med Mol Imaging 2007;34(11):1804–14.

[34] Oliveira EA, Faintuch BL, Núñez EG, Moro AM, Nanda PK, Smith CJ. Radiotracers for different angiogenesis receptors in a melanoma model. Melanoma Res 2012;22(1):45–53.
[35] Babich JW, Fischman AJ. Effect of "co-ligand" on the biodistribution of 99mTc-labeled hydrazino nicotinic acid derivatized chemotactic peptides. Nucl Med Biol 1995;22(1):25–30.
[36] Erfani M, Zarrabi Ahrabi N, Shafiei M, Shirmardi SP. A (99 m) Tc-tricine-HYNIC-labeled peptide targeting the neurotensin receptor for single-photon imaging in malignant tumors. J Labelled Compd Radiopharm 2014;57(3):125–31.
[37] Gandomkar M, Najafi R, Shafiei M, Mazidi M, Goudarzi M, Mirfallah SH, et al. Clinical evaluation of antimicrobial peptide [(99 m)Tc/Tricine/HYNIC(0)]ubiquicidin 29-41 as a human-specific infection imaging agent. Nucl Med Biol 2009;36(2):199–205.
[38] Faintuch BL, Santos RLSR, Souza ALFM, Hoffman TJ, Greeley M, Smith CJ. 99mTc-HYNIC-Bombesin (7–14)NH2: radiochemical evaluation with co-ligands EDDA (EDDA = ethylenediamine-N, N' diacetic acid), tricine, and nicotinic acid. Synth React Inorg Met-Org Nano-Metal Chem 2005;35:43–51.
[39] Liu Z, Wang F. Dual-targeted molecular probes for cancer imaging. Curr Pharm Biotechnol 2010;11:610–9.
[40] Li ZB, Wu Z, Chen K, Ryu EK, Chen X. 18 F-labeled BBN-RGD heterodimer for prostate cancer imaging. J Nucl Med 2008;49:453–61.
[41] Liu Z, Yan Y, Chin FT, Wang F, Chen X. Dual integrin and gastrin-releasing peptide receptor targeted tumor imaging using 18 F-labeled PEGylated RGD-bombesin heterodimer 18 F-FB-PEG3-Glu-RGD-BBN. J Med Chem 2009;52(2):425–32.
[42] Yang J, Guo H, Galazzi F, Berwick M, Padilla RS, Miao Y. Evaluation of a novel Arg-Gly-Asp-conjugated r-Melanocyte stimulating hormone hybrid peptide for potential melanoma therapy. Bioconjug Chem 2009;20:1634–42.
[43] Yang J, Guo H, Miao Y. Technetium-99 m-labeled Arg-Gly-Asp-conjugated alpha-melanocyte stimulating hormone hybrid peptides for human melanoma imaging. Nucl Med Biol 2010;37(8):873–83.
[44] Lister-James J, Moyer BR, Dean RT. Pharmacokinetic considerations in the development of peptide-based imaging agents. Q J Nucl Med 1997;41:111–8.
[45] Denardo SJ, Yao Z, Lam KM, Song A, Burker PA, Merick GR, et al. Effect of molecular size of pegylated peptide on the pharmacokinetics and tumor targeting in lymphoma-bearing mice. Clin Cancer Res 2003;1(9):38545–645.
[46] Vonarbourg A, Passirani C, Saulnier P, Benoit JP. Parameters influencing the stealthiness of colloidal drug delivery systems. Biomaterials 2006;27(24):4356–73.
[47] Boerman OC, Dams ET, Oyen WJ, Corstens FH, Storm G. Radiopharmaceuticals for scintigraphic imaging of infection and inflammation. Inflamm Res 2001;50:55–6.